ARTICLE NO. 78-1227R

Use of Vortex Discretization in Establishing Weak Shock Diffraction Patterns

M.I.G. Bloor* and R.A. Evans†
University of Leeds, Leeds, England

When a weak plane shock front diffracts around a sharp-edged obstacle, the flow, which involves the sudden acceleration of fluid past a salient edge, is characterized by a spiral shear layer emanating from this edge. The method of vortex discretization, in which the shear layer is replaced by an equivalent system of discrete vortices, is particularly suited to this phenomenon and is the approach used in this paper. The calculation of the flowfield using this method allows the shock diffraction pattern to be determined.

Introduction

PROBLEMS involving the diffraction of shocks around sharp-edged obstacles occur in many physical situations. For instance, when a missile is expelled from a launcher, shock waves are initially formed within the guide tube. On reaching the tube extremities, these waves diffract around the tube lips and an understanding of this process is important when assessing its effect on the surroundings. Other examples of pressing concern are the interaction of shock waves with sharp-cornered buildings and the behavior of shock waves at junctions in high-speed railway tunnels.

A common feature associated with these problems, all of which involve the sudden acceleration of fluid past a sharp-bodied obstruction, is the production of a shear layer from the salient edges. Quite often in these complicated gas-flow problems, the shock fronts may be considered to be weak. That is to say, the velocities associated with the motion induced by the primary shock are fairly small when compared with the local sound speeds. For this type of compressible gas flow, it is well established that for large areas of the induced flow the density variations are sufficiently small to be able to justify an incompressible treatment of those regions. Moreover, for these cases of weak shock diffraction, it has been generally observed that the generation of the accompanying shear layer is well ordered, initially rolling up into a vortex spiral. It is suggested that these unsteady problems are amenable to a simplified treatment based on the method of vortex discretization.

The method of vortex discretization utilizes potential flow theory. Most problems considered are of a two-dimensional nature, and, for these cases, the basis of the method is essentially the replacement of the continuous distribution of vorticity in the shear layer by an equivalent system of discrete line vortices. In this way the unsteady fluid motion can be modeled by calculating the velocities of each vortex element and allowing them to be convected with the fluid, thereby enabling the flowfield to be computed at some later time. More often than not, it is convenient to use mapping techniques in order to deal with awkwardly shaped boundaries which confine the fluid flow. A recent review by Clements[1] draws attention to many of the applications of vortex discretization, as well as giving an historical background to its development.

Because of the ease with which experiments may be performed within a shock tube, it is not surprising to find that a number of experiments have been conducted to investigate the phenomenon of shock diffraction. In particular, the case where the flow has been generated by the passage of a weak plane shock past a perpendicular knife edge situated in a duct, has been studied by a number of workers.[2-4] Although this geometry is somewhat complicated to handle analytically, it does have the advantage that experimental data are readily available for comparison with any theoretical predictions. Consequently, this is the model which will be analyzed in the present paper.

The Flow Model

After the incident shock strikes the perpendicular obstruction, the incident wave is diffracted, being partially transmitted and partially reflected. The shadowgraph in Fig. 1 shows that the transmitted and reflected shocks meet in a triple point. Considering the fluid motion in the region immediately behind this point of wave intersection, it is clear that the observed curved reflected wave has degenerated into a sound wave. The region sandwiched between the wave fronts is dominated by a sprial shear layer extending from the knife edge. It has been observed previously that the flow structure initially remains geometrically similar at different times. Such motions, with no obvious characteristic length scale, are termed pseudosteady. A theoretical solution for the rotational flow induced by the shear layer based on the pseudosteady principle has been given by Howard and Matthews,[5] although they made no attempt to model the shock diffraction. During their series of experiments, Howard and Matthews confirmed that the flow between the shocks was approximately incompressible for this case. Rott[6] used this simplification in his analysis of the relation between shock diffraction and the generation of vorticity from the edge. This basis was also employed by Evans and Bloor[7] to model the shear layer generated by weak shock diffraction at a knife edge.

The model proposed consists of an infinite two-dimensional channel of width D containing a perpendicular barrier of infinitesimal thickness and height h. The region in the z plane occupied by the fluid is mapped into the upper half of the ζ plane using a Schwarz-Christoffel transformation which, in this particular case, can be integrated to give

$$z=\frac{2D}{\pi}\tanh^{-1}\left(\frac{\zeta^2-1}{\beta^2-1}\right)^{1/2}$$

Presented as Paper 78-1227 at the AIAA 11th Fluid and Plasma Dynamics Conference, Seattle, Wash., July 10-12, 1978; submitted July 28, 1978; revision received April 2, 1979.

Index categories: Computational Methods; Nozzle and Channel Flow; Shock Waves and Detonations.

*Senior Lecturer, Dept. of Applied Mathematical Studies. Member AIAA.

†Research Fellow, Dept. of Applied Mathematical Studies.

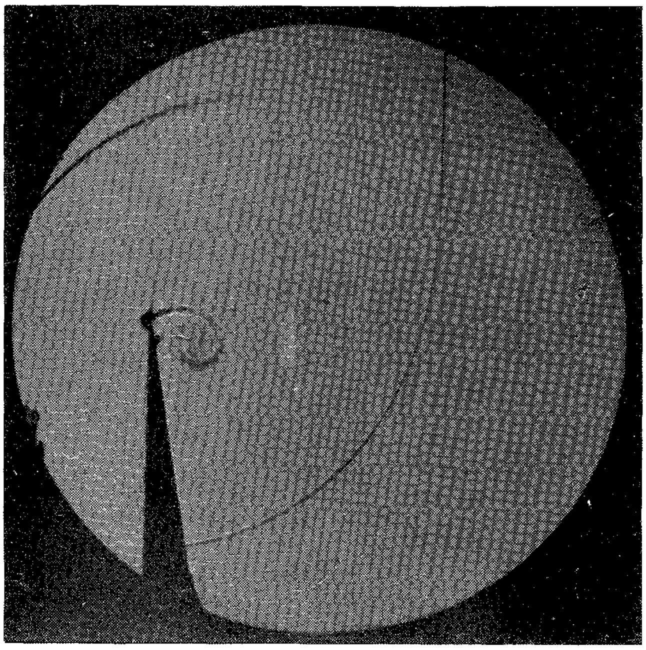

Fig. 1 Shadowgraph of the generation of spiral shear layer following weak shock diffraction at a knife edge.

where $\beta = \pm \operatorname{cosec}(\pi h/2D)$ corresponds to the transformed points at infinity. The geometry is represented in Fig. 2, which shows the correspondence between the physical and transformed planes.

To model the arrival of the plane shock front at the obstruction, the flow is started impulsively and maintained by introducing a source-sink combination at the points at infinity. It is clear from Crocco's theorem that the amount of vorticity subsequently introduced by the curved diffracted shock is of third order in shock strength. Therefore, providing that the incident shock front is weak, it is legitimate to ignore the contributions of vorticity from this source, and only take account of the vorticity shed from the knife edge. This was simulated by introducing discrete elemental vortices into the flow from the tip of the obstruction, their strength k_j and positions z_j being determined from the use of combined Kutta and rate of vorticity shedding conditions.

The region occupied by the fluid in the z plane was transformed to the upper half of the ζ plane and complex potential theory was used to determine the flowfield. Thus, at some general time t_n the complex potential in the transformed plane, taking account of the image system, is given by:

$$\omega(\zeta) = -\frac{DU}{\pi}\log\left(\frac{\zeta+\beta}{\zeta-\beta}\right) + \frac{i}{2\pi}\sum_{j=1}^{n} k_j \log\left(\frac{\zeta-\zeta_j}{\zeta-\bar{\zeta}_j}\right)$$

where U is the magnitude of the induced flow through the channel, and ζ_j the positions of the elemental vortices in the transformed plane. Since the vortex motions in the two planes are not compatible, it was necessary at each time step to return to the physical plane in order to convect the discretized vorticity with the appropriate local velocity using a simple first-order approximation. By carrying out two convective integrations in the period between the release of successive vortices, the accuracy of the integration procedure was improved and no difficulty due to neighboring vortices getting too close was encountered. In this manner, the afterflow was established, being dominated by the rolling up of the shear layer from the tip of the barrier.

Since the flow about the knife edge has been modeled in a realistic manner, it should be possible to infer from these results some of the properties of the shocks that create the flow. That is to say, in the physical problem, the flow produced would have to be compatible with that behind the curved reflected and diffracted shocks. This would suggest that satisfying the usual Rankine-Hugoniot shock conditions would be sufficient to determine the position of the shocks. However, the flow model is incompressible and, under such circumstances, clearly not all the Rankine-Hugoniot conditions can be satisfied. Nevertheless, since the velocities in the flowfield can be claimed to be predicted accurately, these may be used to patch the flow behind the shock, thus predicting the position of the shock separating the two regions. Since the transmitted shock is moving into a stationary gas, the streamlines immediately behind the wave front are orthogonal to it; consequently, the shape of the transmitted shock coincides with a potential line. At any time, the incident wave velocity predicts the position of the shock adjacent to the duct wall and this point on the upper wall boundary serves to determine the particular potential line.

A similar procedure is required to fit the reflected wave, but account must be taken of the fact that the gas ahead of the shock is not at rest in this case. A typical result is illustrated in Fig. 3, where the streamline structure has been incorporated into the diagram to give some insight into the flow pattern. It should be noted that the model contains three density regions which are patched together along velocity discontinuities. Also contained in Fig. 3 is the position of the diffracting waves determined by experiment which allows a comparison

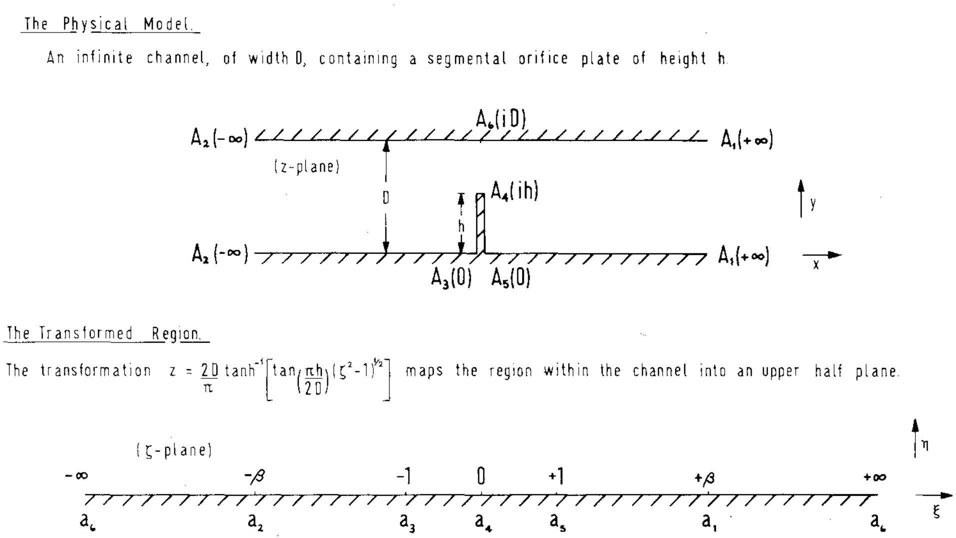

Fig. 2 Correspondence between the physical z plane and the upper half of the ζ plane.

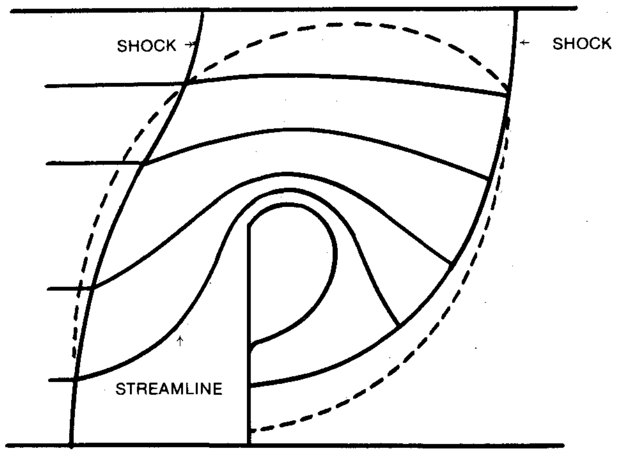

Fig. 3 Streamline pattern and diffracted and reflected shock waves computed from theory. The shock fronts determined from experiment are shown by a dashed line.

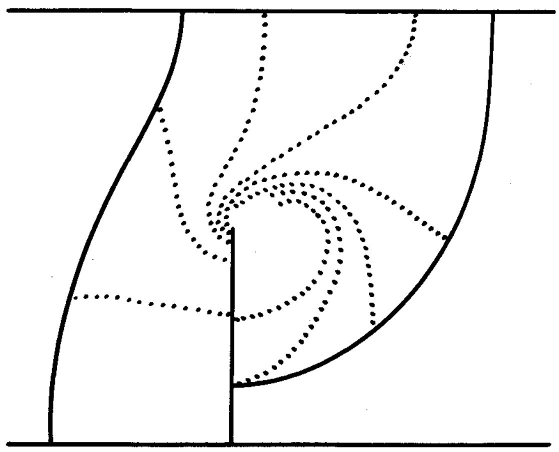

Fig. 4 Calculated pressure distribution: —— wavefronts; ----- isobars, with C_p values (0.8, 0, −0.8, −1.6, −2.4 etc.) taken in a clockwise direction about the edge, starting behind the reflected shock.

to be made. It can be seen that a reasonable approximation of the diffraction pattern is obtained, except for that part of the curved reflected wave in the neighborhood of the triple point. The source of this error is due to the incompressible nature of the model, which clearly means that the presence of the boundaries is communicated instantaneously to all the fluid elements. Consequently, no pseudosteady period of flow is established, contrary to experimental observations, as this is a direct result of the finite-sound speed. Perhaps a better model might be gained by imposing a rate of vorticty shedding based on a similarity principle. Indeed, this approach has been used by Fink and Soh[8] in their recent review to model vortex shedding from a semi-infinite plate. With this method it would be possible to guarantee a self-similar shock pattern, but the later development would be in error.

Usually the quantity of particular physical interest in these problems is the pressure distribution. Furthermore, this provides a direct comparison of the afterflow model with the fully compressible flow.

To obtain a plot of isobars over the flowfield, Bernoulli's equation is used in conjunction with interpolation and a mesh system over the region of interest. Of course, some distortion is produced in the near-field surrounding the rolled-up vortex, but this is of a minor nature. Bernoulli's equation for unsteady incompressible flow is given by:

$$\frac{p}{\rho} + \frac{1}{2}q^2 - \frac{\partial \phi}{\partial t} = g(t)$$

where the unsteady Bernoulli function $g(t)$ is time dependent. At $z=-\infty$, $q=U$ and $p=P_{-\infty}$ say, so that for a known distribution of vorticity, $g(t)$ can be determined in a straightforward manner. In order to calculate the static pressure p, it is necessary to determine the gas velocity q from the complex potential $\omega(\zeta)$, so that the contribution to the total head of the dynamic pressure can be evaluated. In order to determine the time derivative $\partial\phi/\partial t$, it is noted that, since z_j and ζ_j are the only quantities depending on t,

$$\frac{\partial \omega}{\partial t} = \sum_j \left\{ \frac{\partial \omega}{\partial \zeta_j}\frac{\mathrm{d}\zeta_j}{\mathrm{d}z_j}\frac{\mathrm{d}z_j}{\mathrm{d}t} + \frac{\partial \omega}{\partial \bar{\zeta}_j}\frac{\mathrm{d}\bar{\zeta}_j}{\mathrm{d}\bar{z}_j}\frac{\mathrm{d}\bar{z}_j}{\mathrm{d}t} \right\}$$

where

$$\frac{\partial \omega}{\partial \zeta_j} = -\frac{ik_j}{2\pi(\zeta-\zeta_j)}$$

$$\frac{\mathrm{d}\zeta_j}{\mathrm{d}z_j} = \frac{-\pi}{2(\beta^2-1)^{1/2}(\zeta^2-1)^{1/2}} \frac{(\zeta_j^2-\beta^2)(\zeta_j^2-1)}{\zeta_j}$$

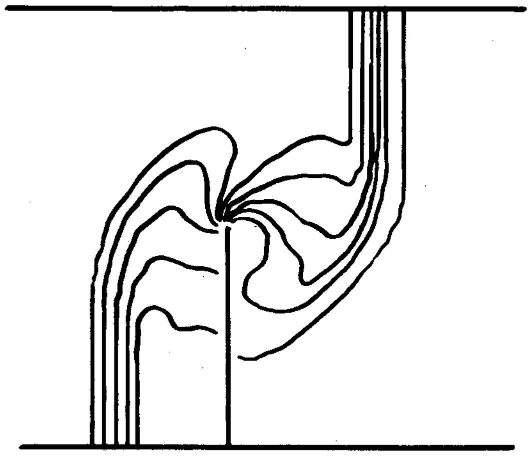

Fig. 5 Isobars in the flowfield using the FLIC method. The values of C_p in the same order as Fig. 4 are 6.58, 4.7, 2.82, 0.94, 0, −0.94, −1.88, −2.82, −3.76, −4.7.

and $\mathrm{d}z_j/\mathrm{d}t$ is the velocity of the jth vortex in the real plane. The resulting pressure distribution is shown in Fig. 4.

Comparison with Other Theoretical Compressible Models

One of the simpler schemes for modeling compressible gas flows that contain shocks is the fluid-in-cell or FLIC method proposed by Gentry et al.[9] more than a decade ago. The method is essentially a two-step Eulerian system in which the compressible flow equations are decoupled to enable the effect of pressure on acceleration and convective effects to be dealt with separately at each time step. The method has been shown to give reasonable qualitative results when comparisons with experiment have been made. With the problem under discussion, Fig. 5 shows the predicted pressure distribution that accompanies a shock diffracted at a vertical plate. The numbers shown in this result correspond to an incident shock strength of about unity. Despite this, the pressure distribution shown in Fig. 4, calculated using the vortex discretization model, shows very favorable agreement in the region behind the transmitted shock. However, behind the reflected shock the errors are indeed large. This is not unexpected since for this shock strength the pressures behind the reflected shock are more than double those predicted by weak shock theory. Even for weak shocks, it seems likely that the accuracy of the incompressible model will be poor, due to the double compression of the gas that takes place in this region.

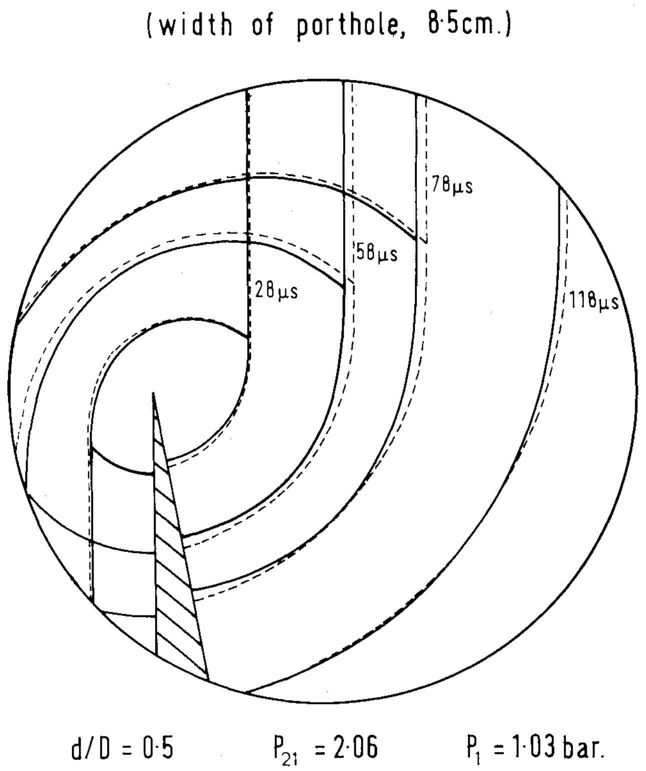

Fig. 6 A comparison of the wavefront results with experiment: —— theory; ----- experiment.

An important point must now be made. In the FLIC scheme fluid viscosity is neglected, although the model does appear to shed vorticity. However, this is fortuitous in that the appearance of a region of vortex flow is due to the introduction of artificial viscosity, which gives rise to a substantial amount of vorticity in regions where high-velocity gradients occur, that is, in the vicinity of the plate tip. Bearing this in mind, the incompressible model is seen to have a stronger theoretical basis. Furthermore, it will be noticed that the shock fronts for the compressible scheme are smeared over several mesh lengths, so that the actual detailed positions of the diffracting wave fronts are lost. This unavoidable effect is again due to the action of artificial viscosity implict in these compressible flow schemes which attempt to model the whole flowfield.

If one is concerned only with the diffracting wave positions, however, shock-smearing can be avoided by using a wave front method related to the pseudo-one-dimensional "ray-tube" approach. The flow in the ray tubes is assumed to be one-dimensional, and, under conditions when the area change along the tube is small, an approximate algebraic relationship between the local shock strength and tube area exists. For the present problem, a calculation was performed following closely the work of Davies and Guy,[10] to whom the reader is referred for more details. Their scheme relies on the pseudosteady development of the wavefront. Very good agreement between experimental observations and the predicted wavefront positions is obtained with this method, as is shown in Fig. 6.

Comparisons between Figs. 3 and 6 indicate the inaccuracy incurred by the incompressible model of shock diffraction. Nevertheless, it must be remembered that the essential feature of the flow, namely the vortex roll-up, is not modeled at all by the ray-tube technique.

Conclusions

Although the use of the vortex discretization model to establish the shock diffraction pattern involves some inaccuracies, especially around the triple point, it is, nevertheless a complete model, in that the shear flow and wave fronts are all predicted. Also, as mentioned earlier, the pressure distribution is usually the feature of interest in the problems, and this is quite accurately predicted by the incompressible model.

It must be pointed out that with the incompressible model, reflections, apart from primary reflection, cannot be handled. However, this criticism also applies in some degree to the other theoretical models mentioned. The wave front method fails to model reflection from the channel wall because the flow behind the incident shock is inaccurately predicted; in particular, there is no vortex. On the other hand, the FLIC method becomes unreliable with many reflections due to the large amount of smearing, that is high artificial viscosity, necessary to maintain stability.

Acknowledgment

This work was supported by Science Research Council Grant GR/A04149, which the authors gratefully acknowledge.

References

[1]Clements, R.R., "Flow Representation Including Separated Regions, Using Discrete Vortices," *AGARD Lecture Series No. 86 on Computational Fluid Dynamics,* 1977, pp. 1-20.

[2]Waldron, H.F., "An Experimental Study of a Spiral Vortex Formed by Shock Wave Diffraction," University of Toronto Institute of Aerophysics, Technical Note 2, 1954.

[3]Schardin, H., "Ein Beispiel zur Verwendug des Stosswellenrohres für Probleme der instationaren Gasdynamik," *Journal of Applied Mathematics and Physics* (ZAMP), Vol. 9, Nov. 1958, pp. 606-621.

[4]Evans, R.A., "A Study of the Starting Mechanism of Wave-Induced Flow Through Orifices in Ducts," Ph.D. Thesis, University of Leeds, England, 1977.

[5]Howard, L.N. and Matthews, D.L., "On the Vortices Produced in Shock Diffraction," *Journal of Applied Physics,* Vol. 27, March 1956, pp. 223-231.

[6]Rott, N., "Diffraction of a Weak Shock Wave with Vortex Generation," *Journal of Fluid Mechanics,* Vol. 1, May 1956, pp. 111-128.

[7]Evans, R.A. and Bloor, M.I.G., "The Starting Mechanism of Wave-Induced Flow Through a Sharp-Edged Orifice," *Journal of Fluid Mechanics,* Vol. 82, Aug. 1977, pp. 115-128.

[8]Fink, P.T. and Soh, W.K., "Calculation of Vortex Sheets in Unsteady Flow and Applications in Ship Hydrodynamics," *Proceedings of the 10th Symposium of Naval Hydrodynamics,* Office of Naval Research, Dept. of Navy, April 1974, pp. 463-491.

[9]Gentry, R.A., Martin, R.E., and Daly, B.J., "An Eulerian Differencing Method of Unsteady Compressible Flow Problems," *Journal of Computational Physics,* Vol. 1, Feb. 1966, pp. 87-98.

[10]Davies, P.O.A.L. and Guy, T.B., "The Prediction of Weak Diffracting and Reflecting Wave Patterns," *Zeitschrift für Flugwissenschaft,* Vol. 19, Heft. 8/9, Sept. 1971, pp. 339-347.